Transition from shear-dominated to Rayleigh-Taylor turbulence

(article starts on next page)

Transition from shear-dominated to Rayleigh–Taylor turbulence*

Stefano Brizzolara[1,2,†], **Jean-Paul Mollicone**[3,4], **Maarten van Reeuwijk**[3], **Andrea Mazzino**[5] and **Markus Holzner**[2,6]

[1]Institute of Environmental Engineering, ETH Zurich, CH-8039 Zurich, Switzerland

[2]Swiss Federal Institute of Forest, Snow and Landscape Research WSL, 8903 Birmensdorf, Switzerland

[3]Department of Civil and Environmental Engineering, Imperial College London, London SW7 2AZ, UK

[4]Division of Fluid Dynamics, Department of Mechanics and Maritime Sciences, Chalmers University of Technology, SE-41296 Gothenburg, Sweden

[5]DICCA, University of Genova and INFN, Genova Section, Via Montallegro, 1, 16145 Genova, Italy

[6]Swiss Federal Institute of Aquatic Science and Technology Eawag, 8600 Dübendorf, Switzerland

Turbulent mixing layers in nature are often characterised by the presence of a mean shear and an unstable buoyancy gradient between two streams of different velocities. Depending on the relative strength of shear versus buoyancy, either the former or the latter may dominate the turbulence and mixing between the two streams. In this paper, we present a phenomenological theory that leads to the identification of two distinct turbulent regimes: an early regime, dominated by mean shear, and a later regime dominated by buoyancy. The main theoretical result consists of the identification of a cross-over timescale that distinguishes between the shear- and the buoyancy-dominated turbulence. This cross-over time depends on three large-scale constants of the flow, namely, the buoyancy difference, the velocity difference between the two streams and the gravitational acceleration. We validate our theory against direct numerical simulations of a temporal turbulent mixing layer compounded with an unstable stratification. We observe that the cross-over time correctly predicts the transition from shear- to buoyancy-driven turbulence, in terms of turbulent kinetic energy production, energy spectra scaling and mixing layer thickness.

Key words: shear layer turbulence, stratified turbulence

1. Introduction

Combined shear-driven and Rayleigh–Taylor (RT) turbulence occurs in mixing layers when the overlying stream is more dense than the underlying one. This configuration results in a complex flow, in which the turbulent mixing process is driven by both shear and buoyancy forces. Examples of such a flow can be found in the natural environment, e.g. in the ocean or the atmosphere (Turner 1979), as well as in industrial processes, e.g. combustion chambers (Nagata & Komori 2000) and inertial confined fusion targets (Atzeni & Meyer-ter Vehn 2004). The two pertinent phenomena, RT and shear-driven turbulence, have been widely studied independently. The RT turbulence phenomenology was originally introduced by Chertkov (2003) and has been recently reviewed by Boffetta & Mazzino (2017). By shear-driven turbulence, here we refer to shear turbulent mixing layers (see Pope (2001), chap. 5, § 5.4.2 for a complete overview).

Only a few works have investigated the compound effect of shear and buoyancy in the mixing of two fluids. In this context, most of the past research was devoted to analysis of the instability phase, referred to as RT/Kelvin–Helmholtz instability (RTKHI), especially in plasma physics (Satyanarayana *et al.* 1984; Finn 1993; Shumlak & Roderick 1998) but also in classical fluid flows (Olson *et al.* 2011). The major result of this research is that, while a linear stability analysis predicts that adding an arbitrary shear velocity to an RT configuration will increase the perturbation growth rate, if early nonlinear effects are taken into account, the shear can lead to a decrease of the growth rate or, *in extremis*, to a suppression of the RTKHI (Shumlak & Roderick 1998; Olson *et al.* 2011).

Focusing on the fully developed turbulent phase, Snider & Andrews (1994) performed an experimental study in a water channel, in which an unstable thermal stratification is combined with a mean shear. The authors inferred that this problem is governed by two different types of transition: one from laminar flow to self-similar turbulence, and the other from shear-driven to buoyancy-driven mixing. Focusing on the latter, the authors identified as a suitable parameter for distinguishing between these two distinct mixing regimes the (negative) bulk Richardson number $Ri = -hg\Delta\rho/(\rho\Delta U^2)$ (where h is mixing layer thickness, $\Delta\rho$ and ρ are the density difference and the reference density, respectively, ΔU is the shear velocity and g is the gravitational acceleration). However, their estimate for the transitional Richardson number spans a wide range, from -5 to -11. Moreover, the transition to turbulence seemed to always occur in the RT regime, and it was not possible to clearly identify the shear-dominated phase. More recent experiments performed in a gas tunnel focused on the later time of the instability phase (Akula, Andrews & Ranjan 2013; Akula *et al.* 2017). The authors identified two distinct mixing regimes through analysis of the mixing layer growth rate, which is expected to be constant for shear-dominated turbulence (Pope 2001, constant velocity) and linear for RT turbulence (Boffetta & Mazzino 2017, constant acceleration). Again, the bulk Richardson number was chosen to be the parameter for identifying the transition from the shear to the RT regime. The transitional Ri was shown to be within the range $(-2.5, -1.5)$ in Akula *et al.* (2013) and $(-2.5, -0.8)$ in Akula *et al.* (2017). However, the range of investigated stratification levels is completely different from that in Snider & Andrews (1994), which might suggest that the transitional Richardson number depends on the stratification level. Moreover, the value of Ri depends sensitively on the definition of the mixing layer thickness h.

The complexity of the transition from shear-dominated to RT turbulence motivated investigators to devise low-order Reynolds-averaged turbulence models to adequately describe it. Within this context, Morgan, Schilling & Hartland (2018) recently proposed a two-length-scale turbulence model to describe compound shear and RT mixing.

Within this framework, the bulk Richardson number is again employed to quantify the relative strength of shear and buoyancy forces.

Despite the effort devoted to this research, only a few of the aforementioned works clearly capture a shear-driven, fully developed turbulent regime, because the investigated shear velocity Reynolds numbers are usually smaller or comparable to those needed for this regime to manifest. In fact, the focus of Akula *et al.* (2013, 2017) and Snider & Andrews (1994) was always stated to be on the (at most) later stage of the instability phase; this is highlighted by the reference time chosen to scale the phenomena ($\sqrt{2\rho H/(\Delta\rho g)}$), which is suitable for quantifying the advancement of the RT instability only. Another critical point regarding the previously mentioned works concerns the so-called early nonlinear phase of the RT instability (Waddell, Niederhaus & Jacobs 2001; Celani *et al.* 2009). During the weakly nonlinear phase of the RT instability, the perturbation growth rate is expected to be constant. Because of this, distinguishing between the early nonlinear RT and the shear-driven turbulence is extremely challenging, especially in laboratory experiments, where a large separation between the time/space at which the transition to turbulence occurs and the time/space at which the transition from shear-dominated to RT turbulence occurs is hard to achieve. Moreover, small-scale quantities (such as the spatial velocity gradient), which could provide suitable indicators of the dominant flow regime, are difficult to access experimentally.

In this work, we investigate the fully developed turbulence arising in unstable stratified mixing layers. Our aim is to (i) clarify in which conditions a transition from shear-dominated to RT turbulence can occur and (ii) provide a phenomenological theory valid for a shear to RT transition where the shear-dominated turbulence is already developed from early times. Finally, we validate our theory against direct numerical simulations of a turbulent temporal mixing layer compounded with an unstable temperature stratification.

2. Phenomenological theory

In the following, we present a phenomenological theory that describes the transition from shear-driven to RT turbulence in a temporal mixing layer, for the case where the flow is already turbulent during the shear-dominated regime. Our theory leads to the identification of a cross-over time, which distinguishes between the shear-dominated and the RT regimes. We assume that the fluid motion is governed by the Navier–Stokes equations with the Boussinesq approximation, i.e. density variations are neglected for inertial effects, while they are still significant in the gravitational term:

$$\frac{\partial \boldsymbol{u}}{\partial t} + \boldsymbol{u} \cdot \boldsymbol{\nabla} \boldsymbol{u} = -\frac{1}{\rho_0}\boldsymbol{\nabla} p + \nu\nabla^2\boldsymbol{u} + \beta g\theta\boldsymbol{e}_3, \tag{2.1}$$

$$\boldsymbol{\nabla} \cdot \boldsymbol{u} = 0, \tag{2.2}$$

where $\boldsymbol{u} = (u, v, w)$ is the fluid velocity in the streamwise, spanwise and wall-normal directions, respectively, θ is the relative temperature, β is the thermal expansion coefficient, g is the gravitational acceleration and ∇^2 is the Laplace operator. The relative temperature is a scalar field that must satisfy the following advection–diffusion equation:

$$\frac{\partial \theta}{\partial t} + \boldsymbol{u} \cdot \boldsymbol{\nabla}\theta = \kappa\nabla^2\theta, \tag{2.3}$$

where κ is the thermal diffusivity.

We consider the case of a temporal turbulent mixing layer. Note that a temporal mixing layer is a limit of the spatial mixing layer for which the ratio between the shear velocity ΔU (the velocity difference between the two streams) and the mean convective velocity U_C (the mean velocity of the two streams) is much less than unity. In such a limit, the flow becomes statistically one-dimensional for an observer travelling in the streamwise direction at the mean convective velocity (Pope 2001, chap. 5, § 5.4.2). Such a flow was experimentally observed to hold for a velocity ratio of at least 0.60 between the two streams (Bell & Mehta 1990), and was numerically reproduced using periodic boundary conditions in the streamwise direction (Rogers & Moser 1994). We assume that the Reynolds number is large enough such that the flow is dominated by large-scale quantities only and the present turbulent state is independent of the initial perturbation and of viscosity. Moreover, we assume that at early times the turbulence is shear-dominated, so that the balance of the Navier–Stokes equation at large scale dictates that the first term on the left-hand side of (2.1) is balanced by the nonlinear term:

$$\frac{u_L}{t} \sim \frac{u_L^2}{h(t)}, \tag{2.4}$$

where u_L is the large-scale velocity magnitude and $h(t)$ is the integral scale that we identify with a measure of the mixing layer thickness. If we assume $u_L \sim \Delta U > 0$ (as is the case for shear-driven turbulence), the well-known linear law for the growth of the mixing layer thickness is thus obtained:

$$h(t) = S\Delta U t. \tag{2.5}$$

The proportionality constant S has been measured both experimentally and numerically, and ranges from 0.06 to 0.11 (Pope 2001). Let us now assume that the flow is gravitationally unstable, i.e. the density of the upper layer is greater than the density of the underlying one. The large-scale balance becomes

$$\underbrace{\frac{\partial \boldsymbol{u}}{\partial t}}_{u_L/t} + \underbrace{\boldsymbol{u} \cdot \boldsymbol{\nabla} \boldsymbol{u}}_{u_L^2/h(t)} = \cdots + \underbrace{\beta g \theta \boldsymbol{e}_3}_{\beta g \Delta \theta}, \tag{2.6}$$

where $\Delta\theta$ is the constant temperature difference between the two streams and the dots on the right-hand side represent the subleading terms. If shear turbulence develops at an early time, it must initially dominate with the scaling of (2.5). The order of magnitude of the inertial term decreases as t^{-1}, and it therefore follows from (2.6) that, sooner or later, the constant on the right-hand side must dominate. This happens when

$$t \simeq t_c \simeq \frac{\Delta U}{\beta g \Delta \theta}. \tag{2.7}$$

For $t \gg t_c$ the buoyancy term becomes dominant; thus, given that always $h(t) \sim u_L t$, the terms on the left-hand side balance the buoyancy term such that

$$\frac{u_L}{t} \sim \beta g \Delta \theta, \tag{2.8}$$

from which one can estimate the large-scale velocity as $u_L \sim \beta g \Delta \theta t$. One can thus obtain the typical RT turbulence law for the mixing layer thickness as $h(t) \sim u_L t$, namely,

$$h(t) = \alpha \beta g \Delta \theta t^2, \tag{2.9}$$

where α has been measured both experimentally and numerically, and ranges from 0.03 to 0.07 (Boffetta & Mazzino 2017).

The same analysis can be conducted from an alternative point of view. Assuming that shear initially dominates turbulent mixing, the governing parameters are ΔU and t, and in this phase self-similarity leads to $h(t) \sim \Delta U t$. The ratio between the buoyancy and inertial forces is described by the bulk Richardson number $Ri = \beta g \Delta \theta h(t) / \Delta U^2$. By imposing $Ri = 1$, one obtains $t_c = t|_{Ri=1} = \Delta U / (\beta g \Delta \theta)$. For later times, the only relevant factors are $\beta g \Delta \theta$ and t, so that the self-similarity of the flow implies $h(t) \sim \beta g \Delta \theta t^2$ and $u_L = \sqrt{\beta g \Delta \theta h(t)}$, which represents the free-fall velocity.

When studying this flow configuration, past research focused on traditional non-dimensional quantities, namely, the large-scale Reynolds number $Re = u_L h(t) / \nu$, the Rayleigh number $Ra = \beta g \Delta \theta h(t)^3 / (\nu \kappa)$ and the Richardson number $Ri = \beta g \Delta \theta h(t) / \Delta U^2$. All these parameters are time-dependent and are thus not suitable for describing the overall behaviour of the system given a set of dimensional flow parameters (initial conditions, boundary conditions and fluid properties). By considering the functional relation between dimensional quantities, namely, $h = f(\Delta U, \beta g \Delta \theta, k, \nu, t)$, in light of our phenomenological theory, we apply the Buckingham-Π theorem using ΔU and t_c as characteristic scales, and reduce the problem to the following relation between non-dimensional quantities:

$$\frac{h}{h_c} = \hat{f}\left(Re_c, \frac{\nu}{\kappa}, \frac{t}{t_c}\right),\tag{2.10}$$

where t_c is the cross-over time defined in the previous section, $h_c = \Delta U t_c$ is the order of magnitude of the corresponding turbulent mixing layer cross-over thickness (assuming shear scaling from early times), $Re_c = \Delta U h_c / \nu$ is the large-scale Reynolds number at transition and $Pr = \nu / \kappa$ is the Prandtl number. The non-dimensional mixing layer thickness, h/h_c, coincides with the bulk Richardson number:

$$\frac{h(t)}{h_c} = \frac{h(t)}{t_c \Delta U} = \frac{h(t) \beta g \Delta \theta}{\Delta U^2} = \frac{h(t) \Delta \rho g}{\rho \Delta U^2} = Ri,\tag{2.11}$$

because $\beta \Delta \theta = \Delta \rho / \rho$. Note that in the Boussinesq approximation $\Delta \rho / \rho = 2A$, where A is the Atwood number.

The classical mixing layer thickness Reynolds number can be expressed as $Re = Re_c \, Ri$, while the Rayleigh number is $Ra = Re_c \, Pr \, Ri$. In contrast to the standard approach, in our formulation Ri is the dependent variable. We can therefore formulate the problem in terms of the following non-dimensional variables:

$$t^* = \frac{t}{t_c}, \quad x^* = \frac{x}{h_c}, \quad u^* = \frac{u}{\Delta U}, \quad p^* = \frac{p}{\rho_0 \Delta U^2}, \quad \theta^* = \frac{\theta}{\Delta \theta},\tag{2.12a–e}$$

which transform the momentum equation (2.1), continuity equation (2.2) and scalar transport equation (2.3) to

$$\frac{\partial u^*}{\partial t^*} + u^* \cdot \nabla u^* = -\nabla p^* + \frac{1}{Re_c} \nabla^2 u^* + \theta^* e_3,\tag{2.13}$$

$$\nabla \cdot u^* = 0,\tag{2.14}$$

$$\frac{\partial \theta^*}{\partial t^*} + u^* \cdot \nabla \theta^* = \frac{1}{Re_c \, Pr} \nabla^2 \theta^*.\tag{2.15}$$

A critical aspect that we clarify with our theory concerns the existence of the shear-dominated turbulent phase. By assuming that the shear initially dominates, we assert

that our theory holds under the condition that the turbulence is already fully developed in the shear-driven regime. The reason why this is a necessary condition lies in the fact that our theory requires the global flow behaviour to be governed from early times by large-scale flow parameters only, i.e. to be independent of the viscous scales. Considering (2.10), this condition requires that the cross-over Reynolds number Re_c be much larger than the shear-driven transition-to-turbulence Reynolds number, Re_s. The latter is the Reynolds number at which the mixing layer reaches a fully developed turbulent state in the absence of stratification. The value of Re_s is documented to depend on various factors, namely: (i) the velocity ratio, (ii) the density ratio, (iii) the initial shear-layer profile and in particular (iv) the shape and nature of the instability. It can vary over a wide range (3000–17 000) (Bernal & Roshko 1986; Koochesfahani & Dimotakis 1986). In the case of uniform density, the temporal mixing layer limit is the one for which the shear-driven transition-to-turbulence Reynolds number is generally smaller (Breidenthal 1981), so that, in our case, we can in principle rely on the lower limit.

3. Direct numerical simulations

The temporal mixing layer is simulated by imposing periodic boundary conditions in the streamwise and spanwise directions, while a free-slip condition is imposed on the lower and upper walls. The streamwise velocity profile and the scalar concentration field are initialised with step functions $u = \Delta U \operatorname{sign}(z)/2$ (Rogers & Moser 1994) and $\theta = \Delta\theta/2(\operatorname{sign}(z) + 1))$, respectively. Equations (2.1), (2.2) and (2.3) are solved with a fourth-order-accurate finite-volume spatial discretisation scheme and a third-order Adams–Bashforth scheme for time integration (Verstappen & Veldman 2003; Craske & van Reeuwijk 2015). We fixed $Pr = \nu/\kappa = 1$ for all the simulations. We also fixed $\Delta U = 1$ and $\Delta\theta = 1$, and changed the control parameter Re_c to act on the kinematic viscosity ν and on the coefficient β. As shown in § 2, Re_c is indeed the only control parameter for this problem. We checked *a posteriori* that a sufficiently wide range of t/t_c were explored, in order to be certain to observe the transition between shear-dominated and RT turbulence. In addition to the non-dimensional parameters discussed in § 2, table 1 also lists the ratio t_c/t_0, where t_0 is the time at which the mixing layer would reach a developed turbulent state in the absence of stratification, i.e. $\beta = 0$. In particular, t_0 is the time at which the following two conditions are met: (i) $Re_\lambda \geq 50$ and (ii) a $\sim k^{-5/3}$ spectrum with at least one decade of wavenumber separation being visible. The first three most stratified simulations (*SL*1, *SL*2 and *SL*3) were initialised with laminar initial conditions. In these cases, the cross-over Reynolds number is small, so that the transition to turbulence is triggered directly by RT. The time t_0 required for shear-dominated transition to turbulence to occur was evaluated by performing a simulation with no buoyancy (*SNB*) and the same viscosity as in *SL*1, *SL*2 and *SL*3. For the three less stratified cases *ST*4, *ST*5 and *ST*6, Re_c is significantly higher, meaning that the transition to turbulence is expected to occur earlier than the transition from shear to RT turbulence. In these cases we decided to switch on the buoyancy term at t_0, that is, when the turbulence has already developed because of shear. This is equivalent to initialising the simulations with an already shear-triggered turbulent flow. This precaution, which can be realised in numerical simulations only, ensures shear-dominated turbulence at t_0, avoiding, at the same time, the ambiguity between shear turbulent mixing and early nonlinear RT instability, which characterised the previous experiments conducted with comparable shear and buoyancy forcing. The latter reasoning allows us to overcome the problem of having moderately high shear

Label		$L_xL_yL_z$	$N_xN_yN_z$	$Re_c = \Delta U^3/(\beta g\Delta\theta\nu)$	t_c/t_0	t_{end}/t_c
SL1	■	96^3	2160^3	1.06×10^3	0.04	19.63
SL2	◆	96^3	2160^3	4.00×10^3	0.15	7.81
SL3	▲	96^3	2160^3	7.99×10^3	0.30	5.21
ST4	★	$96^2 \times 192$	$1080^2 \times 2160$	6.25×10^4	3.33	2.30
ST5	✳	$96^2 \times 192$	$1080^2 \times 2160$	6.95×10^4	3.58	5.99
ST6	●	$96^2 \times 192$	$1080^2 \times 2160$	1.04×10^5	5.00	1.60
SNB	—	96^3	2160^3	∞	∞	0

Table 1. Simulation parameters: L_i and N_i denote the size and the number of grid points along the ith direction, respectively; Re_c is the Reynolds number corresponding to the cross-over time; t_0 is the time at which the flow with shear only would reach a fully developed turbulent state (i.e. $Re_\lambda \geq 50$ and a clear scale separation in the turbulent spectra); t_c is the cross-over time as predicted by (2.7); t_{end} is the total time of each simulation.

Reynolds numbers, which imposes both experimental-facility limitations and constraints on the computational power requirements of direct numerical simulations. Table 1 also lists the ratio between the total simulation time t_{end} and the cross-over time t_c, showing that all the simulations reach the buoyancy-dominated phase.

4. Results and discussion

To check the tendency of the flow to attain asymptotically the RT-like structure, we rely on the following argument: consider the Nusselt number $Nu = \langle w'\theta'\rangle h(t)/(k\Delta\theta)$, i.e. the ratio between the total turbulent scalar transport and the diffusive transport (the angled brackets indicate the average within the mixing layer), and the Reynolds number $Re = u_L h(t)/\nu$. By assuming RT-like scaling $u_L = \beta g\theta t$ and $h \sim \beta g\Delta\theta t^2$, we obtain the following relations:

$$Nu \sim Ra^{1/2}Pr^{1/2}, \qquad Re \sim Ra^{1/2}Pr^{-1/2}, \qquad (4.1a,b)$$

where $Ra = \beta g\Delta\theta h(t)^3/(\nu\kappa)$ is the Rayleigh number (a dimensionless measure of the density difference). This state is sometimes referred to as the ultimate state of convection in the case of Rayleigh–Bénard (RB) convection (Kraichnan 1962); it is expected to appear at very large Rayleigh numbers, when boundary layers break down and the scalar and momentum mixing is driven by large-scale contributions (Lohse & Toschi 2003). While this regime hardly emerges in RB turbulence because of the important role played by the boundaries, in RT configurations it is clearly manifest (Boffetta *et al.* 2012). Thus, these scaling laws are a good method for checking the tendency of the flow to reach RT turbulence. From here on, we consider the temperature integral thickness $h_\theta = \int_{-\infty}^{+\infty} 4\theta(1-\theta)\,\mathrm{d}z$ (Vladimirova & Chertkov 2009) as a proxy for the mixing layer thickness $h(t)$. We chose this quantity instead of the momentum thickness (which is usually employed in mixing layer theory) because the latter is suitable for shear mixing layers only, while the temperature thickness is still suitable for quantifying the mixing width in both limits. We recall that in our simulations, the Prandtl number $Pr = \kappa/\nu$ is fixed at 1. Figure 1 shows clearly that all the simulated cases converge asymptotically to the scaling $(Nu, Re) \sim Ra^{1/2}$, regardless of the initial stratification.

Different characteristic quantities of the flow can be analysed to discern between shear- and buoyancy-driven turbulence. The most direct way to quantitatively check the validity of our theory is to analyse the turbulent kinetic energy (*tke*) balance. We chose the integral
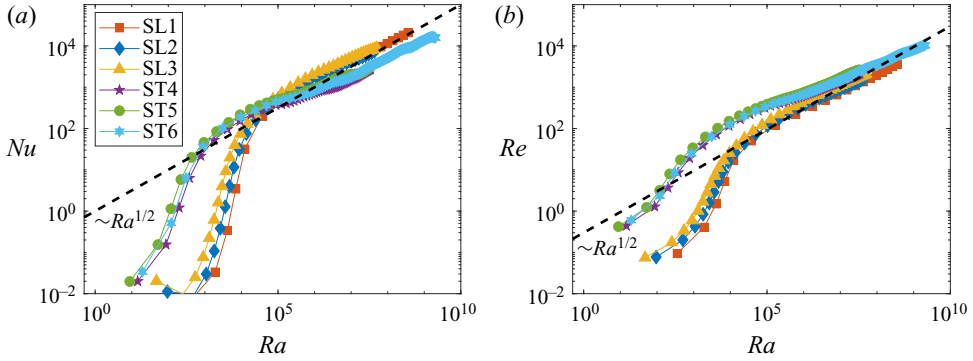
Figure 1. Ultimate state scaling as a check for the turbulence to reach the buoyancy-dominated regime:
(a) Nu vs Ra; (b) Re vs Ra; Pr is fixed at 1.

tke balance (integrated over the wall-normal direction), because this does not depend on the definition of the mixing layer thickness $h(t)$. The *tke* integral balance is written

$$\frac{\partial E}{\partial t} + \varepsilon = \mathcal{P}_B + \mathcal{P}_G, \tag{4.2}$$

where $E = \int_{-\infty}^{+\infty} (\overline{\boldsymbol{u}' \cdot \boldsymbol{u}'})^2 / 2 \, dz$ is the *tke* per unit mass, $\varepsilon = \nu \int_{-\infty}^{+\infty} \overline{(\nabla \boldsymbol{u}')^2} \, dz$ is the viscous dissipation, $\mathcal{P}_B = \beta g \int_{-\infty}^{+\infty} \overline{w'\theta'} \, dz$ is the buoyancy production and $\mathcal{P}_G = -\int_{-\infty}^{+\infty} \overline{w'u'} \partial_z \bar{u} \, dz$ is the gradient production; the overline represents the horizontal average. Initially, when shear dominates ($t < t_c$), *tke* is mainly produced by $\mathcal{P}_G$, i.e. the ratio between the buoyancy and the shear production is smaller than unity. In this phase, the gradient production balances the dissipation rate ($\partial E/\partial t + \varepsilon \sim \mathcal{P}_G$). For later times, buoyancy overcomes shear, i.e. the dissipation rate is balanced by buoyancy as in pure RT turbulence ($\partial E/\partial t + \varepsilon \sim \mathcal{P}_B$). In more detail, when $t < t_c$, we expect that $u_L \sim \Delta U$ and $h(t) \sim \Delta U t$ for both $\mathcal{P}_B$ and $\mathcal{P}_G$. Indeed, the buoyancy production term is expected to be passively transported by the shear velocity without any relevant influence of the buoyancy force. For later times, we expect the variation of the streamwise mean velocity to be shear-dominated, i.e. $\partial \bar{u}/\partial z \sim \Delta U/h(t)$. The latter assertion is reasonable, because in temporal mixing layers $(\bar{v}, \bar{w}) = (0, 0)$, while in pure RT turbulence $\bar{u} = 0$. The streamwise mean velocity derivative is thus expected to be mostly affected by the shear velocity scale. Concerning the wall-normal turbulent flux, we assume that $u' \sim \Delta U$ and $w' \sim \beta g \Delta \theta$, such that $\overline{u'w'}$ scales as $\Delta U (\beta g \Delta \theta) t$, i.e. the Reynolds stress tensor remains anisotropic for longer times. We found this to agree well with our data (inset of figure 2a). Note that this is not the case for pure RT turbulence, in which the mean shear is absent. The scale of variation of the mean streamwise velocity can be identified using any measure of the mixing layer thickness. However, it is not needed to derive the scaling of $\mathcal{P}_G$, because it drops out after integration along the wall-normal direction. Consequently, we obtain the following scalings for the shear and buoyancy *tke* production:

$$\mathcal{P}_G \sim \begin{cases} \Delta U^3 & \text{if } t \ll t_c, \\ (\beta g \Delta \theta) \Delta U^2 t & \text{if } t \gg t_c, \end{cases} \quad \mathcal{P}_B \sim \begin{cases} (\beta g \Delta \theta) \Delta U^2 t & \text{if } t \ll t_c, \\ (\beta g \Delta \theta)^3 t^3 & \text{if } t \gg t_c, \end{cases} \tag{4.3a,b}$$

which implies that the flux Richardson number $Ri_f = \mathcal{P}_B/\mathcal{P}_G \sim t$ for $t \ll t_c$ and $\mathcal{P}_B/\mathcal{P}_G \sim t^2$ for $t \gg t_c$. Figure 2(a) shows that our phenomenological prediction
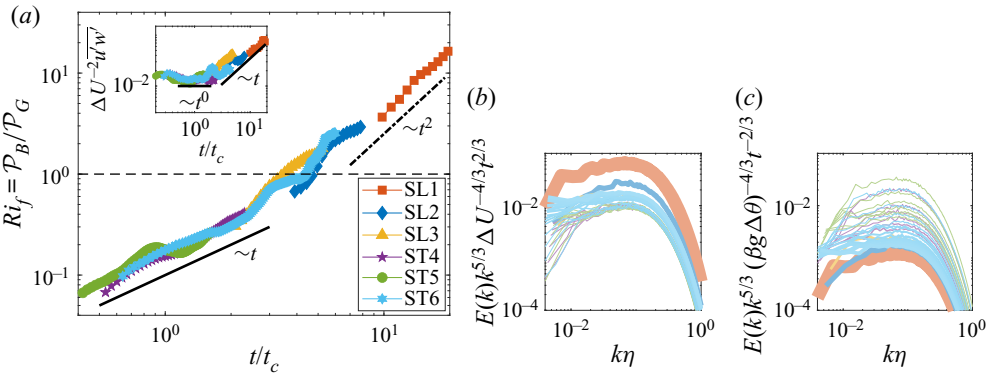
924 A10-8

Figure 2. Temporal scalings of the turbulent kinetic energy: (*a*) ratio between the buoyancy and gradient *tke* production (i.e. the flux Richardson number Ri_f) integrated over the wall-normal direction, with the inset showing the scaling of $\overline{u'w'}$ at the centreline; energy spectra normalised with the (*b*) shear and (*c*) RT scalings for all the simulations (see (4.4)); the line thickness is proportional to the non-dimensional time.

reasonably matches the data in the limits of $t \ll t_c$ and $t \gg t_c$. As predicted, the shear-dominated phase clearly appears only in *ST*4, *ST*5 and *ST*6, for which Re_c is high, and thus the transition from laminar to self-similar turbulence is shear-dominated. In the strongly stratified cases (*SL*1, *SL*2 and *SL*3), the shear-dominated turbulence is suppressed, because the buoyancy term already prevails during the transition to turbulence (low Re_c). A noteworthy consideration is that, considering even the simulations in which the shear-driven turbulence is inhibited, the flux-Richardson number scaling still holds when considering only the turbulent phase.

Another argument relies on the temporal scaling of the energy spectra. By considering *K*41 inertial scaling (Kolmogorov [1941](#), [1962](#); Obukhov [1941*a*](#), [*b*](#), [1962](#)), one can derive two different scaling behaviours for the second-order structure function or, equivalently, the energy spectra. In terms of energy spectra, RT and shear turbulence are expected to scale equally with the wavenumber k, but differently with time (see Boffetta & Mazzino ([2017](#)) for a complete discussion on the energy spectra temporal scaling in three-dimensional RT turbulence). Simple power counting leads to the following spectral scalings:

$$E(k) \sim \begin{cases} \Delta U^{4/3} t^{-2/3} k^{-5/3} & \text{if } t \ll t_c, \\ (\beta g \Delta\theta)^{4/3} t^{2/3} k^{-5/3} & \text{if } t \gg t_c, \end{cases} \tag{4.4}$$

[Figure 2](#)(*b*,*c*) shows that shear/RT scaling holds for early/late times, respectively. Indeed, all the curves tend to stabilise on RT-like spectra for later non-dimensional times (thick line), and the shear scaling holds for early non-dimensional times (thin line), while becoming unreliable for later non-dimensional times (thicker line).

Finally, the two regimes can also be distinguished by analysing the bulk Richardson number $h(t)/h_c$ and the mixing layer growth rate $\delta h(t)/\delta t$. In the shear-dominated phase a linear spreading of the mixing layer is expected, while when buoyancy prevails the mixing region grows quadratically. In other words, the mixing layer growth rate is expected to be constant in the shear-dominated phase and linear in the RT phase. Despite the fact that this method is the one usually adopted to distinguish between the two regimes, it often does not provide clear evidence of the dominance of shear over buoyancy, and *vice versa*. The reason is that the tendency of the mixing layer to grow linearly or quadratically is not a
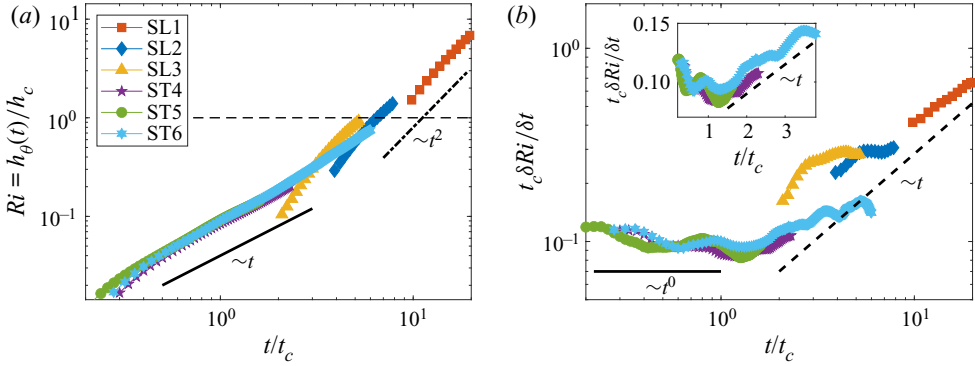
924 A10-9

Figure 3. Bulk Richardson number (*a*) and bulk Richardson number growth rate (*b*); the inset shows *ST*4, *ST*5 and *ST*6 in linear space; note that the bulk Richardson number growth rate is a non-dimensional measure of the mixing layer thickness growth rate, because h_θ is proportional to *Ri*.

direct measure of the predominance of one forcing over the other, but only a consequence, that is, not directly causally correlated to the phenomena (in support of this argument, one may consider the early nonlinear phase of RT). Figure 3(*a*) shows that, as expected, *Ri* grows linearly for $t \ll t_c$ and quadratically for $t \gg t_c$. Figure 3(*b*) shows $\delta h(t)/\delta t$ for *ST*4, *ST*5 and *ST*6, where an initial constant-like behaviour, which becomes linear near $t = t_c$ is appreciable, while *SL*1, *SL*2 and *SL*3 show only a linear trend, meaning that the shear-dominated turbulent phase is suppressed. The inset of figure 3(*b*), shows the growth rate in linear space for *ST*4, *ST*5 and *ST*6, highlighting the transitional phase between shear-dominated and RT turbulence.

Having shown that the cross-over time t_c correctly scales the bulk and the flux Richardson numbers, one may be interested in the exact value of the non-dimensional time at which the transition effectively occurs, $t/t_c|_T$. To estimate $t/t_c|_T$ we adopt the following procedure for *Ri*, Ri_f and $t_c \delta Ri/\delta t$. Firstly, we fit the phenomenological asymptotic predictions for $t \ll t_c$ and $t \gg t_c$ into the early and late-time data of *Ri*, Ri_f and $t_c \delta Ri/\delta t$. This is done systematically, by increasing the distance from $t/t_c = 1$ until the constant fitting coefficients no longer change. Then, the transitional time is estimated as the intersection between the two fitted asymptotic laws. For instance, by considering the bulk Richardson number, we expect $Ri = b_{shear} (t/t_c)^1$ at early times and $Ri = b_{RT} (t/t_c)^2$ for later times; b_{shear} and b_{RT} are evaluated using the aforementioned fitting procedure, and the transitional time is obtained as $t/t_c|_T = b_{shear}/b_{RT}$. Table 2 lists the values of $t/t_c|_T$ for each of the considered observables, together with their corresponding values at each of the transitional times. We report also the value of the gradient Richardson number evaluated at the centreline ($Ri_g = (-g/\rho \partial \bar{\rho}/\partial z)/(\partial \bar{u}/\partial z)^2$ at $z = 0$) and the corresponding transitional time.

We frame our results in the context of past research. By analysing the results of Akula *et al.* (2013, 2017), we evaluate the control parameter Re_c to identify experiments that are likely to include a shear-dominated turbulent regime. A notable case is experiment *A2S2*, in which $Re_c \simeq 17\,000$. Akula *et al.* (2017) evaluated the transitional location by analysing the mixing layer growth rate and then estimated Ri_g at the centreline at that location. We can thus compare their value of Ri_g at the transition with line three, column four of table 2: Akula *et al.* (2017) obtained $Ri_g = 0.17$ in experiment *A2S2*, which is almost equal to our estimate ($Ri_g = 0.18$). Again, considering the mixing layer growth rate, experiment

924 A10-10

	$t/t_c|_T$	$Ri(t/t_c|_T)$	$Ri_f(t/t_c|_T)$	$Ri_g(t/t_c|_T, z = 0)$
Ri	4.66	0.40	0.34	0.79
Ri_g	5.82	0.42	0.42	0.99
$t_c\, \delta Ri/\delta t$	2.47	0.21	0.42	0.18
Ri_f	3.81	0.64	0.28	0.65

Table 2. Transitional time for each observable and the corresponding Richardson numbers. Column one lists the transition times $t/t_c|_T$ for the bulk, gradient (at the centreline), increment and flux Richardson numbers. Columns two to four list the values of Ri, $Ri_f(z = 0)$ and Ri_g at the corresponding transitional time in column one.

$A2S2$ transitions from shear-dominated to RT turbulence at $t/t_c|_T = 2.09$, which is close to the value 2.47 listed in table 2 (column one, line three). This further confirms that the cross-over time t_c correctly predicts the transition from shear- to buoyancy-dominated turbulence for sufficiently high Re_c (turbulence already developed in the shear-dominated phase). Moreover, t_c is shown to correctly scale the time even when the shear-dominated phase is suppressed, provided that only the fully developed turbulent phase is considered.

5. Concluding remarks

In this work, we have systematically analysed the problem of transition from shear-dominated to Boussinesq RT turbulence through theory and the use of direct numerical simulations. Our phenomenological approach allows us to predict a cross-over time $t_c \simeq \Delta U/(\beta g \Delta \theta)$ at which an initially shear-dominated turbulent flow transitions to RT turbulence. The direct numerical simulations confirmed the validity of our theory, in particular in terms of the flux Richardson number, a direct measure of which factor dominates the turbulence (buoyancy or shear). Moreover, using the Buckingham-Π theorem, we clarified in which conditions the shear-dominated turbulence is suppressed (low values of Re_c). This latter aspect is particularly noteworthy, because it highlights the fact that only when the turbulence is fully developed at early times is it reasonable to expect the flow to show universal behaviour (i.e. the transition at a unique non-dimensional time).

In § 4, we derived a scaling law for the flux Richardson number that is in good agreement with the data. This follows from the non-trivial scaling $\overline{u'w'} \sim \Delta U(\beta g \theta)t$, i.e. that the Reynolds stress tensor remains anisotropic also for longer times. This scaling is expected to have implications for turbulence modelling, because in pure RT turbulence $\overline{u'w'}$ is always equal to zero. For instance, it follows from our framework that the eddy viscosity is not constant in time and should feature an explicit dependence on the growing impact of stratification also for later times when the unstable stratification dominates the turbulence.

At the end of § 4 we framed our work in the context of past research. By comparing our results with the experiment of Akula *et al.* (2017), we observe that at large Re_c, there may be a well-defined value of $t/t_c|_T$ (approximately 2.5) as well as of the transitional gradient Richardson number (approximately 0.18). In other words, while for small values of Re_c we expect a more complex dependency of $t/t_c|_T$ and $Ri_g(t/t_c|_T, z = 0)$ on the control parameter Re_c (and eventually on the nature of the perturbation), at finite but large Re_c a unique and universal value of $t/t_c|_T$ (or $Ri_g(t/t_c|_T, z = 0)$) may exist. This fact is crucial, given that the Reynolds numbers are usually large in many natural environments as well as in industrial applications. The detailed study of this aspect is left to future work.

924 A10-11

Declaration of interests. The authors report no conflict of interest.

Author ORCIDs.

ⓘ Jean-Paul Mollicone https://orcid.org/0000-0002-8989-4762;

ⓘ Maarten van Reeuwijk https://orcid.org/0000-0003-4840-5050;

ⓘ Andrea Mazzino https://orcid.org/0000-0003-0170-2891;

ⓘ Markus Holzner https://orcid.org/0000-0003-2702-8612.

REFERENCES

AKULA, B., ANDREWS, M.J. & RANJAN, D. 2013 Effect of shear on Rayleigh–Taylor mixing at small Atwood number. *Phys. Rev.* E **87** (3), 033013.

AKULA, B., SUCHANDRA, P., MIKHAEIL, M. & RANJAN, D. 2017 Dynamics of unstably stratified free shear flows: an experimental investigation of coupled Kelvin–Helmholtz and Rayleigh–Taylor instability. *J. Fluid Mech.* **816**, 619–660.

ATZENI, S. & MEYER-TER VEHN, J. 2004 *The Physics of Inertial Fusion: Beam Plasma Interaction, Hydrodynamics, Hot Dense Matter*. Oxford University Press.

BELL, J.H. & MEHTA, R.D. 1990 Development of a two-stream mixing layer from tripped and untripped boundary layers. *AIAA J.* **28** (12), 2034–2042.

BERNAL, L.P. & ROSHKO, A. 1986 Streamwise vortex structure in plane mixing layers. *J. Fluid Mech.* **170**, 499–525.

BOFFETTA, G., DE LILLO, F., MAZZINO, A. & VOZELLA, L. 2012 The ultimate state of thermal convection in Rayleigh–Taylor turbulence. *Physica* D **241** (3), 137–140.

BOFFETTA, G. & MAZZINO, A. 2017 Incompressible Rayleigh–Taylor turbulence. *Annu. Rev. Fluid Mech.* **49**, 119–143.

BREIDENTHAL, R. 1981 Structure in turbulent mixing layers and wakes using a chemical reaction. *J. Fluid Mech.* **109**, 1–24.

CELANI, A., MAZZINO, A., MURATORE-GINANNESCHI, P. & VOZELLA, L. 2009 Phase-field model for the Rayleigh–Taylor instability of immiscible fluids. *J. Fluid Mech.* **622**, 115–134.

CHERTKOV, M. 2003 Phenomenology of Rayleigh–Taylor turbulence. *Phys. Rev. Lett.* **91** (11), 115001.

CRASKE, J. & VAN REEUWIJK, M. 2015 Energy dispersion in turbulent jets. Part 1. Direct simulation of steady and unsteady jets. *J. Fluid Mech.* **763**, 500–537.

FINN, J.M. 1993 Nonlinear interaction of Rayleigh–Taylor and shear instabilities. *Phys. Fluids* B*: Plasma Phys.* **5** (2), 415–432.

KOLMOGOROV, A.N. 1941 The local structure of turbulence in incompressible viscous fluid for very large Reynolds numbers. *C. R. Acad. Sci. URSS* **30**, 301–305.

KOLMOGOROV, A.N. 1962 A refinement of previous hypotheses concerning the local structure of turbulence in a viscous incompressible fluid at high Reynolds number. *J. Fluid Mech.* **13** (1), 82–85.

KOOCHESFAHANI, M.M. & DIMOTAKIS, P.E. 1986 Mixing and chemical reactions in a turbulent liquid mixing layer. *J. Fluid Mech.* **170**, 83–112.

KRAICHNAN, R.H. 1962 Turbulent thermal convection at arbitrary Prandtl number. *Phys. Fluids* **5** (11), 1374–1389.

LOHSE, D. & TOSCHI, F. 2003 Ultimate state of thermal convection. *Phys. Rev. Lett.* **90** (3), 034502.

MORGAN, B.E., SCHILLING, O. & HARTLAND, T.A. 2018 Two-length-scale turbulence model for self-similar buoyancy-, shock-, and shear-driven mixing. *Phys. Rev.* E **97** (1), 013104.

NAGATA, K. & KOMORI, S. 2000 The effects of unstable stratification and mean shear on the chemical reaction in grid turbulence. *J. Fluid Mech.* **408**, 39–52.

OBUKHOV, A.M. 1941*a* On the distribution of energy in the spectrum of turbulent flow. *Bull. Acad. Sci. USSR Geog. Geophys.* **5**, 453–466.

OBUKHOV, A. 1941*b* Spectral energy distribution in a turbulent flow. *Izv. Akad. Nauk. SSSR. Ser. Geogr. i. Geofiz* **5**, 453–466.

OBUKHOV, A.M. 1962 Some specific features of atmospheric turbulence. *J. Geophys. Res.* **67** (8), 3011–3014.

OLSON, B.J., LARSSON, J., LELE, S.K. & COOK, A.W. 2011 Nonlinear effects in the combined Rayleigh–Taylor/Kelvin-Helmholtz instability. *Phys. Fluids* **23** (11), 114107.

POPE, S.B. 2001 *Turbulent Flows*. Cambridge University Press.

ROGERS, M.M. & MOSER, R.D. 1994 Direct simulation of a self-similar turbulent mixing layer. *Phys. Fluids* **6** (2), 903–923.

SATYANARAYANA, P., GUZDAR, P.N., HUBA, J.D. & OSSAKOW, S.L. 1984 Rayleigh–Taylor instability in the presence of a stratified shear layer. *J. Geophys. Res.* **89** (A5), 2945–2954.

SHUMLAK, U. & RODERICK, N.F. 1998 Mitigation of the Rayleigh–Taylor instability by sheared axial flows. *Phys. Plasmas* **5** (6), 2384–2389.

SNIDER, D.M. & ANDREWS, M.J. 1994 Rayleigh–Taylor and shear driven mixing with an unstable thermal stratification. *Phys. Fluids* **6** (10), 3324–3334.

TURNER, J.S. 1979 *Buoyancy Effects in Fluids*. Cambridge University Press.

VERSTAPPEN, R.W.C.P. & VELDMAN, A.E.P. 2003 Symmetry-preserving discretization of turbulent flow. *J. Comput. Phys.* **187** (1), 343–368.

VLADIMIROVA, N. & CHERTKOV, M. 2009 Self-similarity and universality in Rayleigh–Taylor, Boussinesq turbulence. *Phys. Fluids* **21** (1), 015102.

WADDELL, J.T., NIEDERHAUS, C.E. & JACOBS, J.W. 2001 Experimental study of Rayleigh–Taylor instability: low Atwood number liquid systems with single-mode initial perturbations. *Phys. Fluids* **13** (5), 1263–1273.